



Cutting Force Modeling in a Three-Axis Milling Process Based on Cutting Tool – Workpiece Interaction

Nhu-Tung Nguyen¹(✉), Pham Duc Cuong¹, and Gia-Thinh Bui²

¹ HaUI Institute of Technology, Hanoi University of Industry, Hanoi, Vietnam
tungnn@hauai.edu.vn

² Department of Electrical and Mechanical Engineering, Hai Phong University, Haiphong, Vietnam

Abstract. In this paper, based on the interaction between workpiece and cutting tool, the cutting forces (CFs) in the three-axis milling process were modeled using linear cutting force models (CFMs) and the short line segment volume following the toolpath. In the three-axis milling process, many short line segment volumes were separated from the toolpath. In each short line segment volume, the average axial cutting depth (a), radial cutting depth (b), direction angle (θ), feed rate (f), and so on were calculated. Based on these calculated input parameters, the CFs were modeled and compared with the measured CFs. Several milling tests were performed to verify the proposed CFMs in the three-axis milling process. The predicted CFs were quite close to measured CFs both in the amplitude and the shape.

Keywords: CFs · Milling · Three-axis milling · Cutting process · Toolpath · Modeling

1 Introduction

In the milling process, the CF is one of the most important factors to determine the machining characteristics and improve the quality and effectiveness of the machining processes. Two approaches that are applied to model the cutting force in the milling process are the experimental investigation approach [1, 2] and the theoretical approach [3, 4]. The advantages and disadvantages of each approach were considered to apply for each specific case. The experimental investigation approach is not difficult to implement and gives good results merely applied to a specific case. The conclusions drawn from the experimental investigation approach have little or no general applicability. This approach was applied in several previous studies to predict the cutting forces milling processes [5, 6]. Using this approach, most of the models used to predict the CFs in milling processes are regression analysis models based on the experimental data from a large number of experiments and only apply for specific cases [4–7].

In the theoretical approach, a big disadvantage of this approach is a lot of factors that need to be considered when modeling the cutting forces such as tool geometry, tool wear,

tool deflections, certain thermal phenomena, vibrations, etc. So, to increase prediction accuracy, these factors have to be integrated into the cutting force model. Although this approach is not easy to apply, it has been implemented by various researchers because the obtained results can be characterized as fairly good with general applicability [8, 9]. Moreover, using this approach, the cutting force models can be developed step by step by integrating more machining condition factors into the previous models. Most of the studies focus on modeling the cutting force when milling following a straight line with a short cutting time. The cutting force models will be verified over several revolutions of the cutting tool. This execution method is applicable to milling using a flat mill tool [10], a ball mill tool [11], or a face mill tool [12]. This study was carried out to model the cutting force when milling following a toolpath based on the interaction between the cutting tool and the workpiece.

2 Modeling of CFs in Three-Axis Milling Process

2.1 Modeling of CFs

In three-axis milling processes, the CFs at each cutter position (P_i) (x, y, z coordinates) were described as in Fig. 1. According to the coordinate transformation, CFs were calculated by Eq. (1).

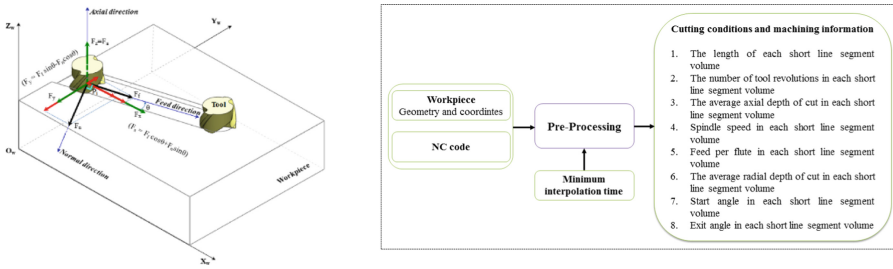


Fig. 1. CFs in three-axis milling process

$$\begin{Bmatrix} F_x \\ F_y \\ F_z \end{Bmatrix} = \begin{Bmatrix} F_f \cos \theta + F_n \sin \theta \\ F_f \sin \theta - F_n \cos \theta \\ F_a \end{Bmatrix} \quad (1)$$

Equation (1) can be applied to predict CFs for a short tool path with the constant cutting depth, constant feed rate, constant cutting angle, etc. So, based on a minimum interpolation time, a long toolpath was divided into many very small elements (short line segment volume). With each element, the cutting conditions (cutting depth, feed rate, cutting angle, etc.) were constants and were determined by the calculation process as described in Fig. 1.

2.2 Calculation Process of Input Parameters

a. Feed per Flute Calculation

From the NC program with spindle speed (S), federate (F), and the tool information (number of flutes), the feed per flute was calculated by Eq. (2).

$$f_t = \frac{F}{SN_f} \quad (2)$$

where N_f is the number of flutes in the tool.

b. Calculation of cutting depth and direction angle

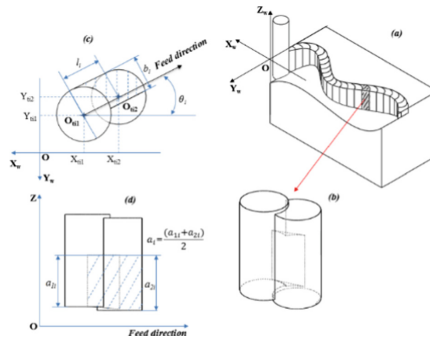
The average axial cutting depth (a_i) and direction angle (θ_i) of each short line segment volume in XY plane were presented in and calculated by Eq. (3) and Eq. (4) as shown in Fig. 2

$$a_i = \frac{a_{i1} + a_{i2}}{2} \quad (3)$$

where a_{i1} and a_{i2} are the axial cutting depth of short line segment volume number i and $i + 1$.

$$\theta_i = \tan^{-1} \left(\frac{Y_{ii2} - Y_{ii1}}{X_{ii2} - X_{ii1}} \right) \quad (4)$$

where (X_{ii1}, Y_{ii1}) and (X_{ii2}, Y_{ii2}) are the coordinates of center point of tool in two nearest positions (O_{ii1} and O_{ii2}) as shown in Fig. 2.



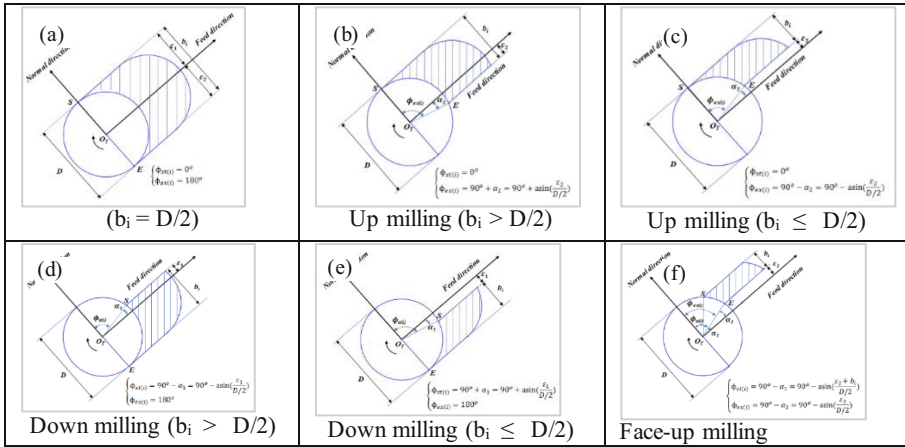
(a) Short line segment; (b) Geometry of short line segment volume; (c) Direction angle; (d) Axial cutting depth

Fig. 2. Interaction short line segment volume of tool and workpiece

c. Start and exit angle calculation

The start and exit angle in each cutter rotation were calculated based on the comparison of cutter diameter and radial cutting depth as described in Table 1.

Table 1. Calculation of start and exit angle with different radial cutting depth



3 Experimental Method

3.1 Experimental Tool, Workpiece, Machine, and Measurement System

To verify the CFMs, several experiments were performed with different cutting conditions. A flat mill tool was used in the experimental process with the properties as listed in Table 2.

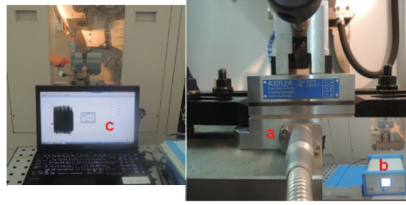
Table 2. Properties of experimental cutting tool

D (mm)	L (mm)	N _f	β (deg)	α (deg)	γ (deg)	Cutter type	Material
10	80	2	30	5	5	Flat-end mill	HSS-Co

Aluminum alloy Al6061-T6 workpiece was used in the experimental process with the sizes of 80 mm × 40 mm × 40 mm and the properties as following: hardness = 95 HB, Young’s modulus = 68.9 GPa, Poisson’s ratio = 0.33, tensile strength = 310 MPa.

The TMV-510C three-axis CNC milling machine was used in the cutting test with several specifications as follow: X/Y/Z axis stroke of 510/360/300 mm, X/Y/Z axis rapid of 48/48/48 m/min, and the maximum spindle speed of 8000 rpm.

A KISTLER dynamometer system (Type 9257B, SN 4565813) was used to measure the CFs in experimental process as illustrated in Fig. 3. The DynoWare software was used to analyze and display the CF signals.



a. CF sensor b. Data processing box c. PC and software

Fig. 3. CF measurement system

3.2 Experimental Machining Conditions

The cutting tests were conducted following a short straight line and following a tool path to verify the CFMs. The cutting conditions for this experiment were listed in the Table 3.

Table 3. Cutting conditions

a (mm)	f_t (mm/flute)	F (mm/min)	S (rpm)	Cutting type
0.5	0.1	200	1000	Straight line (slotting)
0.6	0.05	200	2000	Toolpath (slotting)

4 Experimental Results and Discussion

4.1 CFs in Several Cutter Rotation

In the case of milling following a short straight line, the predicted and measured CFs were described in Fig. 4. This fig showed that the predicted CFs were quite close to the measured ones in all feed, normal, and axial directions. So, in this case, the predicted and measured results of CFs had a good agreement with both the amplitude and the shape of CFs.

4.2 CFs Following a Toolpath

In the case of milling following a toolpath, the comparison of the predicted and measured CF was described in Fig. 5. The amplitude of predicted CFs is sometimes larger and sometimes smaller than the amplitude of measured cutting forces. However, the shapes of cutting forces are quite the same as the measured CFs. So, in this study, although, exiting some different points between predicted CFs and measured CFs, the differences are not so much. Besides, the shape of the predicted CFs was also quite close to the measured one. Above all, the predicted result of the proposed three-axis CFMs are quite close to the measured ones. Therefore, these proposed CFMs can be used to predict the CFs in three-axis milling processes.

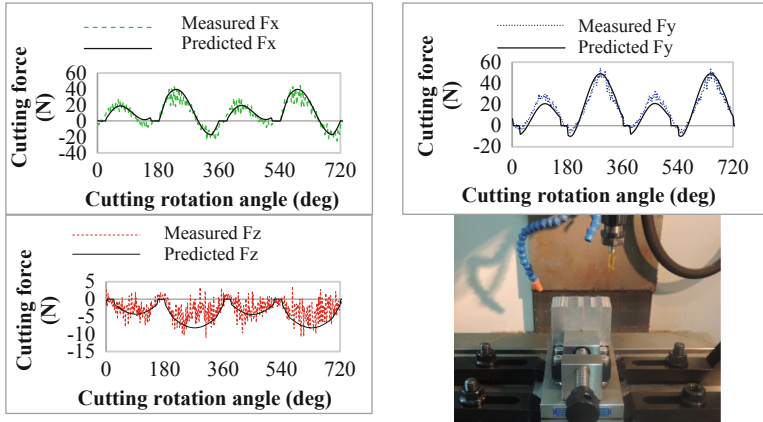


Fig. 4. CFs when milling following a short straight line

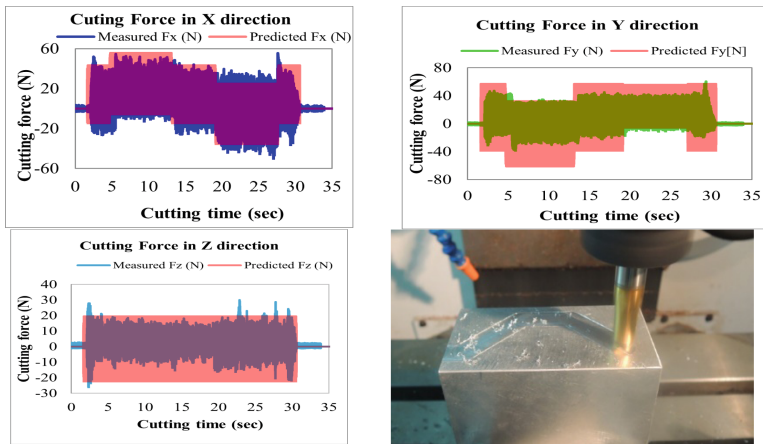


Fig. 5. CFs when milling following a toolpath

5 Conclusion

The conclusions were drawn in this study as follows:

- CFs in the three-axis milling process were modeled using linear CFMs and the short line segment volume following the toolpath.
- The toolpath in the three-axis milling process can be divided into many short line segment volumes with the constant values of axial cutting depth (a), radial cutting depth (b), feed rate (f), direction angle (θ), etc.
- Both amplitude and shape of predicted CFs were quite close the that one of measured CFs.
- Develop the CFMs when milling following a complex profile will be one of the further research directions of this study.

References

1. Hoang, T.D., Nguyen, N.T., Tran, D.Q., Nguyen, V.T.: Cutting forces and surface roughness in face-milling of SKD61 hard steel. *Strojnicki Vestnik J. Mech. Eng.* **65**(6), 375–385 (2019). <https://doi.org/10.5545/sv-jme.2019.6057>
2. Imani, L., Henzaki, A.R., Hamzeloo, R., Davoodi, B.: Modeling and optimizing of cutting force and surface roughness in milling process of Inconel 738 using hybrid ANN and GA. In: *Proceedings of the Institution of Mechanical Engineers Part B: Journal of Engineering Manufacture*, vol. 234, no. 5, pp. 920–932 (2020). <https://doi.org/10.1177/0954405419889204>
3. Nguyen, N.-T., Kao, Y.-C., Dung, H.T., Trung, D.D.: A prediction method of dynamic cutting forces and machine-tool vibrations when milling by using ball-end mill cutter. In: Sattler, K.-U., Nguyen, D.C., Vu, N.P., Tien Long, B., Puta, H. (eds.) *ICERA 2019. LNNS*, vol. 104, pp. 47–54. Springer, Cham (2020). https://doi.org/10.1007/978-3-030-37497-6_5
4. Agarwal, A., Desai, K.A.: Importance of bottom and flank edges in force models for flat-end milling operation. *Int. J. Adv. Manuf. Technol.* **107**(3–4), 1437–1449 (2020). <https://doi.org/10.1007/s00170-020-05111-5>
5. Turgut, Y., Çinici, H., Sahin, I., Findik, T.: Study of cutting force and surface roughness in milling of Al/Sic metal matrix composites. *Sci. Res. Essays* **6**(10), 2056–2062 (2011). <https://doi.org/10.5897/SRE10.496>
6. Shankar, S., Mohanraj, T., Rajasekar, R.: Prediction of cutting tool wear during milling process using artificial intelligence techniques. *Int. J. Comput. Integr. Manuf.* **32**(2), 174–182 (2019). <https://doi.org/10.1080/0951192X.2018.1550681>
7. Sahoo, P., Pratap, T., Patra, K.: A hybrid modelling approach towards prediction of cutting forces in micro end milling of Ti-6Al-4V titanium alloy. *Int. J. Mech. Sci.* **150**, 495–509 (2019). <https://doi.org/10.1016/j.ijmecsci.2018.10.032>
8. Kao, Y.-C., Nguyen, N.-T., Chen, M.-S., Su, S.-T.: A prediction method of cutting force coefficients with helix angle of flat-end cutter and its application in a virtual three-axis milling simulation system. *Int. J. Adv. Manuf. Technol.* **77**(9–12), 1793–1809 (2014). <https://doi.org/10.1007/s00170-014-6550-8>
9. Rubeo, M.A., Schmitz, T.L.: Milling force modeling: a comparison of two approaches. *Procedia Manuf.* **5**, 90–105 (2016). <https://doi.org/10.1016/j.promfg.2016.08.010>
10. Wan, M., Lu, M.S., Zhang, W.H., Yang, Y.: A new ternary-mechanism model for the prediction of cutting forces in flat end milling. *Int. J. Mach. Tools Manuf.* **57**, 34–45 (2012). <https://doi.org/10.1016/j.ijmachtools.2012.02.003>
11. Kao, Y.C., Nguyen, N.T., Chen, M.S., Huang, S.C.: A combination method of the theory and experiment in the determination of cutting force coefficients in ball-end mill processes. *J. Comput. Des. Eng.* **2**(4), 233–247 (2015). <https://doi.org/10.1016/j.jcde.2015.06.005>
12. Ghorbani, H., Moetakef-Imani, B.: Specific cutting force and cutting condition interaction modeling for round insert face milling operation. *Int. J. Adv. Manuf. Technol.* **84**(5–8), 1705–1715 (2015). <https://doi.org/10.1007/s00170-015-7985-2>